Hindawi
Oxidative Medicine and Cellular Longevity
Volume 2022, Article ID 4189083, 12 pages
https://doi.org/10.1155/2022/4189083

Research Article

4,7-Didehydro-neophysalin B Protects Rat Lung Epithelial Cells against Hydrogen Peroxide-Induced Oxidative Damage through Nrf2-Mediated Signaling Pathway

Qiu Zhong,[1] Yaogui Sun,[1] Ajab Khan,[2] Jianhua Guo,[3] Zhirui Wang,[4] Na Sun,[1] and Hongquan Li[1]

[1]*Shanxi Key Lab. for Modernization of TCVM, College of Veterinary Medicine, Shanxi Agricultural University, Taigu, 030801 Shanxi, China*
[2]*Department of Veterinary Pathology, Faculty of Veterinary and Animal Sciences, The University of Agriculture, Dera Ismail Khan 29050, Khyber Pakhtunkhwa, Pakistan*
[3]*USA Texas A&M University, College Station, TX, USA 77843*
[4]*University of Colorado Denver Anschutz Medical Campus, RC2-6013, Mail Stop 8621 12700 E 19th Ave., Aurora, CO 80045, USA*

Correspondence should be addressed to Hongquan Li; livets@163.com

Received 4 June 2021; Revised 29 June 2022; Accepted 19 July 2022; Published 12 September 2022

Academic Editor: Anderson J. Teodoro

The administration of 4,7-didehydro-neophysalin B is expected to be a promising strategy for mitigating oxidative stress in respiratory diseases. This study was aimed at investigating the efficacy of 4,7-didehydro-neophysalin B for apoptosis resistance of rat lung epithelial cells (RLE-6TN) to oxidative stress and evaluating its underlying mechanism of action. The RLE-6TN cells treated with hydrogen peroxide (H_2O_2) were divided into five groups, and 4,7-didehydro-neophysalin B was administered into it. To evaluate its mechanism of action, the expression of oxidative stress and apoptotic proteins was investigated. 4,7-Didehydro-neophysalin B significantly inhibited H_2O_2-induced RLE-6TN cell damage. It also activated the Nrf2 signaling pathway which was evident from the increased transcription of antioxidant responsive of KLF9, NQO1, Keap-1, and HO-1. Nrf2 was found to be a potential target of 4,7-didehydro-neophysalin B. The protein levels of Bcl-2 and Bcl-xL were increased while Bax and p53 were decreased significantly. Flow cytometry showed that 4,7-didehydro-neophysalin B protected RLE-6TN cells from apoptosis and has improved the oxidative damage. This study provided a promising evidence that 4,7-didehydro-neophysalin B can be a therapeutic option for oxidative stress in respiratory diseases.

1. Introduction

The respiratory epithelial cell damage is a key indicator of respiratory diseases. Investigation of respiratory epithelial cell injury and its underlying mechanism of action and development of new drugs against it are crucial steps to prevent and treat respiratory diseases. Hydrogen peroxide (H_2O_2) is the main reactive oxygen species (ROS) involved in the regulation of redox reactions in biological activities through specific protein targets [1]. Recently, oxidative stress is considered as a key risk factor for respiratory diseases [2]; evidences showed that the causative factors of diseases including mycoplasma pneumonia are also linked with the oxidative stress [3–6]. Therefore, the active compounds with antioxidative properties tend to be the potential agents for the prevention of respiratory diseases.

In recent years, the use of active natural compounds against pathological conditions has gained considerable recognition. 4,7-Didehydro-neophysalin B and *Physalin* B are biologically active substances extracted from *Physalis alkekengi L. var. franchetii*. It has been confirmed that *Physalin* B has various pharmacological effects such as anti-inflammatory [7], antitumor [8], antibacterial [9], and immune regulation [10] verified by various bioassay both

Table 1: Nrf2 siRNA: a pool of 3 different siRNA duplexes.

siRNA	Primer (5′→3′)
Nrf2 A	Sense: GCAUGCUACGUGAUGAAGAtt Antisense: UCUUCAUCACGUAGCAUGCtt
Nrf2 B	Sense: CUCCUACUGUGAUGUGAAAtt Antisense: UUUCACAUCACAGUAGGAGtt
Nrf2 C	Sense: GUGUCAGUAUGUUGAAUCAtt Antisense: UGAUUCAACAUACUGACACtt

Table 2: Primers used in RT-PCR.

Gene	Primer (5′→3′)
Nrf2	Forward: GAGAGCCCAGTCTTCATTGC Reverse: TTGGCTTCTGGACTTGGAAC
Keap1	Forward: TTCAAGGCCATGTTCACCAA Reverse: TGGATACCCTCAATGGACACC
NQO1	Forward: GGAGAGTTTGCTTACACTTACGC Reverse: AGTGGTGATGGAAAGCACTGCCTTC
HO-1	Forward: CGCCTTCCTGCTCAACATT Reverse: TGTGTTCCTCTGTCAGCATCAC
KLF9	Forward: GGGAAACCTCCGAAAA Reverse: CGTTCACCTGTATGCACTGTA
GAPDH	Forward: GGAGATTACTGCCCTGGCTC Reverse: GACTCATCGTACTCCT

RT-PCR was performed on the ABI PRISM® 7500 real-time PCR analyzer (Applied Biosystems, Foster City, CA, USA) using the SYBR® Premix Ex Taq™ RT-PCR Kit. The relative mRNA expression was calculated by means of $2^{-\Delta\Delta Ct}$ and was normalized to the mean mRNA expressions of GAPDH. The results were calculated with the following formulae: ratio = $2^{-\Delta\Delta Ct}$, $\Delta\Delta Ct = (Ct_{target} - Ct_{GAPDH})_{Sample} - (Ct_{target} - Ct_{GAPDH})_{Control}$.

in vitro and in vivo. 4,7-Didehydro-neophysalin B is a new kind of *Physalin* B lacking two hydrogen atoms. There is evidence that *Physalin* B has efficient antioxidant activity [8]. However, the protective effect and mechanism of 4,7-didehydro-neophysalin B against H_2O_2-induced lung injury remained elusive.

Nuclear factor-erythroid 2-related factor-2 (Nrf2) has been identified as a key regulator of antioxidative, anti-inflammatory, and conjugation/detoxification proteins including NAD(P)H, quinine oxidoreductase 1 (NQO1), and heme oxygenase-1 (HO-1) [11]. After oxidative stress caused by H_2O_2 or other factors, the Nrf2 pathway is rapidly activated to eliminate intracellular ROS generation, thereby attenuating DNA damage induced by H_2O_2 to reduce risk of subsequent lung apoptosis [12].

Activation of antioxidative defense such as phase II enzyme expression is an effective way to protect cells against oxidative damage [13]. Nrf2 combined with antioxidant response element (ARE) system is one of the most important defensive signaling pathways to regulate the transcription activity of antioxidases [14]. The RLE-6TN cell line has been widely used to evaluate lung function due to their hypersensitivity to H_2O_2 [15, 16]. Although many bioactive compounds have been reported against oxidative stress, still there is no relevant study on the cytoprotective effect of 4,7-didehydro-neophysalin B on RLE-6TN cells.

In this study, H_2O_2 was used to establish the basic oxidative damage model so that we can investigate the effect of 4,7-didehydro-neophysalin B on the oxidative stress, cell apoptosis, and the role of Nrf2 signaling pathway. This study will promote the development of nutraceutical and functional food from *Physalis alkekengi L. var. franchetii* or its extracts for reducing the risk of oxidative stress-induced lung injury.

2. Materials and Methods

2.1. Preparation of 4,7-Didehydro-neophysalin B. Physalin was isolated from the stems of *Physalis alkekengi L. var. franchetii*. The plant was identified by Dr. Qiongming Xu from the College of Pharmaceutical Science, Soochow University. Physalin was purified, and the purity of Physalin is 72.39% by chromatography [17]. Physalin from the above reaction was pulverized, extracted with ethanol, loaded on a silica gel column, eluted, and purified with ethyl acetate. The obtained contents of 4,7-didehydro-neophysalin B were detected by chromatography.

2.2. Cytotoxicity of 4,7-Didehydro-neophysalin B. The RLE-6TN cells (ATCC® CRL-2300™, 4000 cells per well) were subcultured in 96-well plates. After different concentrations of 4,7-didehydro-neophysalin B (50, 25, 10, and 5 μg/mL) treatments, cells were incubated with CCK-8 (CK04, Dojindo, Japan) solution (10%) for 1 h at 37°C. The resulting absorbance was measured at 450 nm by using a microplate reader (Tecan, Switzerland). The maximum nontoxic concentration (MNTC) value was calculated by Prism 6 software (San Diego, CA, USA) [18].

$$\text{Cell proliferation rate} = \frac{A_{450} \text{ of treatment group}}{A_{450} \text{ of blank group}} \times 100\%. \quad (1)$$

2.3. Culture of RLE-6TN Cells. The RLE-6TN cell line was cultured in DMEM containing 15% fetal bovine serum, 2 mmol/L glutamine, 5 mmol/L sodium pyruvate, and 25 mmol/L HEPES, containing 100 UI/mL penicillin and 100 μg/mL streptomycin, placed in an incubator and grown at 37°C, 5% CO_2-saturated humidity. 0.25% trypsin-EDTA digested and passaged, and cells in logarithmic growth phase were used for experiments [19]. RLE-6TN cells were seeded in 96-well cell culture plates and incubated in a 5% CO_2 humidified incubator for 24 h at 37°C. Various concentrations of H_2O_2 prepared in 2% medium (200, 100, 50, and 25 μmol) were added and incubated again for 4, 8, 12, and 24 h. The cell proliferation rate of H_2O_2 was determined using the CCK-8 (CK04, Dojindo, Japan) kit. To develop a cellular oxidative damage model, H_2O_2 (100 μmol) prepared in 2% medium was added to each well except the blank group and incubated for the next 12 h. Different concentrations of 4,7-didehydro-neophysalin B with low-dose group (2.5 μg/mL), medium-dose group (5 μg/mL), and high-dose

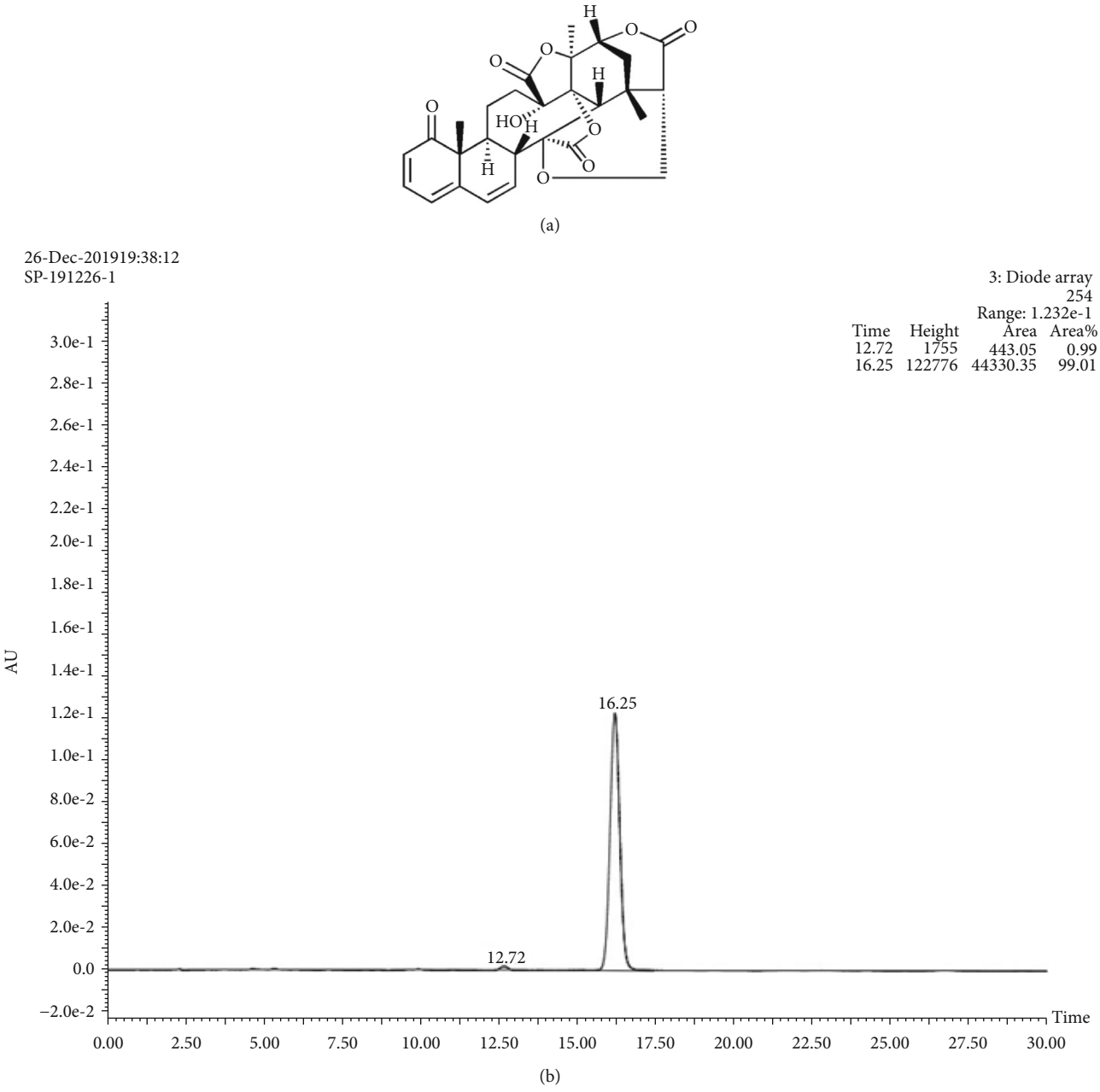

Figure 1: (a) The structure of 4,7-didehydro-neophysalin B. (b) The contents of 4,7-didehydro-neophysalin B.

group (10 μg/mL) were added as treatment and incubated again for 24 h.

$$\text{Cell proliferation rate} = \frac{A_{450} \text{ of treatment group}}{A_{450} \text{ of blank group}} \times 100\%. \quad (2)$$

2.4. Transfection. (1) Culture the RLE-6TN cells for 3 to 5 generations, select the cells with good growth condition, digest the cells with 0.25% trypsin, inoculate 2×10^5 cells/well in 6-well plates, add 10% fetal bovine serum, culture in F12 medium (Gibco, USA) without double antibody for 24 h, and after the cell confluence reached 70%, transfection was carried out. (2) Mix 7.5 μL of Lipofectamine 2000 (Life, USA) with 125 μL of OPTI-MEM (Gibco, USA) medium. Take another EP tube and mix 6 μL of siRNA (0.75 μg) with 125 μL of OPTI-MEM medium. This is the amount for one well in a 6-well plate. (3) Gently mix the two tubes of mixture in step 2, and let them act together at room temperature for 15 min. (4) The liquid after the joint action in step 3 was directly added to the original 6-well plate medium, and after 6 hours in a 37°C, 5% CO_2 incubator, the medium was replaced and the subsequent experiments were carried out. For siRNA transfection, siRNA duplex targeting Nrf2 (sc-37030, Santa Cruz Biotechnology, Santa Cruz, CA, USA, primer shown in Table 1) were used. siRNA (sc-37007, Santa Cruz Biotechnology, Santa Cruz, CA, USA) was selected as a

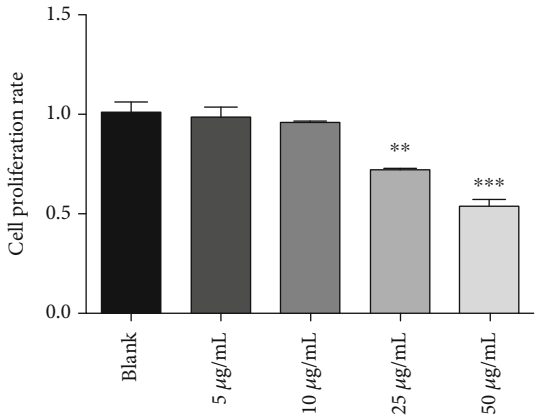

FIGURE 2: Cell viability (CCK-8) assay results of RLE-6TN cells: 4,7-didehydro-neophysalin B-induced cell proliferation rate. Compared with the blank group, $^{*}p < 0.05$, $^{**}p < 0.01$, and $^{***}p < 0.001$.

control to determine whether Nrf2's siRNA was successfully transfected.

2.5. Detection of Gene Expression in Tissues by RT-PCR. The total RNA was extracted from cells using TRIzol reagent, and the absorbance was measured at 260 and 280 nm by an ultraviolet spectrophotometer. The RNA content was calculated from the absorbance (A) value at a wavelength of 260 nm while the RNA purity was identified by the ratio of A_{260}/A_{280}. Reverse transcription of total RNA was performed with reverse transcriptase. The PCR primers (shown in Table 2) were designed and synthesized by KeyGEN BioTECH with GAPDH as endogenous control, and the PCR reactions were carried out according to the recommended conditions.

2.6. Flow Cytometry. After treating the cells with/without 100 μmol of H_2O_2 for 12 h, different concentrations of 4,7-didehydro-neophysalin B (0, 2.5, 5, and 10 μg/mL) were added to the rat lung epithelial cells RLE-6TN for 24 h. The cells were collected, washed twice with cold PBS, and centrifuged at 1000 rpm for 5 min, the supernatant was discarded, and the cells were made into a single cell suspension. 5 μL of Annexin V-FITC and 5 μL PI were added, mixed, and incubated for 15 min in the dark. Finally, 400 μL of binding buffer was added and cell apoptosis was detected using flow cytometry.

2.7. Western Blot. RLE-6TN cells were homogenized with RIPA lysate (Solarbio, Beijing, China) containing protease inhibitor PMSF and phosphatase inhibitor (Solarbio). The nuclear and cytosolic proteins were extracted by a nuclear protein extraction kit (KeyGEN BioTECH, Jiangsu, China). The protein concentrations were measured by bicinchoninic acid (BCA) protein assay kit (Beyotime, Shanghai, China). 40 μg equivalent protein samples were separated by SDS-PAGE gel electrophoresis and were transferred into a polyvinylidene fluoride (PVDF) membrane. The membranes were incubated with appropriate primary and HRP-conjugated secondary antibodies. Chemiluminescence was visualized with an enhanced chemiluminescence kit (BOSTER, Wuhan, China). Glyceraldehyde-3-phosphate dehydrogenase (GAPDH) protein (Sanying, Wuhan, China) and the TATA-binding protein (TBP) (Sanying, Wuhan, China) were used as loading control. The antibodies for Nrf2, heme oxygenase-1 (HO-1), nicotinamide adenine dinucleotide phosphatase:quinone-acceptor 1 (NQO1), Krueppel-like factor 9 (KLF9), Keap-1, p53, Bcl-2-associated X protein (Bax), B cell lymphoma gene 2 (Bcl-2), and B cell lymphoma-extra large (Bcl-xL) were purchased from Abcam (UK). All secondary antibodies were from Sanying (Wuhan, China). Protein expression was analyzed by scanning densitometry using ImageJ software (USA).

To further explain the molecular mechanism by which 4,7-didehydro-neophysalin B treated H_2O_2-induced oxidative damage in RLE-6TN cells, western blot was performed. Nrf2's siRNA was generated to inhibit Nrf2 expression, and the inhibitory efficiency was verified using western blot. Nrf2's siRNA was transfected into RLE-6TN cells with or without H_2O_2 treatment. Then, 10 μg/mL 4,7-didehydro-neophysalin B was administrated for treatment and the expression of Nrf2 was explored using western blotting.

2.8. Statistical Analysis. Statistical analysis was performed by one-way analysis of variance with Tukey's test post hoc comparisons and Student's t-test when comparing between 2 groups using SPSS 19.0 software (USA). The data were presented as the mean ± SEM. Values with $p < 0.05$ was considered statistically significant.

3. Results

3.1. Structure and Content of 4,7-Didehydro-neophysalin B. The structure and contents of 4,7-didehydro-neophysalin B are shown in Figures 1(a) and 1(b). The chemical formula of 4,7-didehydro-neophysalin B is $C_{28}H_{28}O_9$, and its purity is 99.01%.

3.2. The Cytotoxicity of 4,7-Didehydro-neophysalin B. The maximum nontoxic concentration of 4,7-didehydro-neophysalin B in RLE-6TN was investigated. Compared with the blank group, RLE-6TN cells treated with 25 μg/mL 4,7-didehydro-neophysalin B for 24 h showed significant reduction in cell viability (74.87 ± 1.54%, $p = 0.008 < 0.01$) while 10 μg/mL 4,7-didehydro-neophysalin B had negligible effect on cell viability (93.6 ± 1.03%, $p = 0.07 > 0.05$) (Figure 2). Therefore, we choose 10 μg/mL 4,7-didehydro-neophysalin B as the maximum nontoxic concentration.

3.3. The Effect of 4,7-Didehydro-neophysalin B on RLE-6TN Pretreated with H_2O_2. Compared with the blank group, the working concentration for H_2O_2 in RLE-6TN cells treated with different concentrations was determined. Results showed that 100 μmol H_2O_2 treated for 12 h significantly reduced (59.87 ± 1.32%, $p = 0.0004 < 0.001$) while 50 μmol H_2O_2 showed less effect on the cell viability (80.37 ± 1.96% , $p = 0.0007 < 0.001$). The mortality of cells treated with 200 μmol of H_2O_2 was too high (41.28 ± 2.84%, $p = 0.0003$

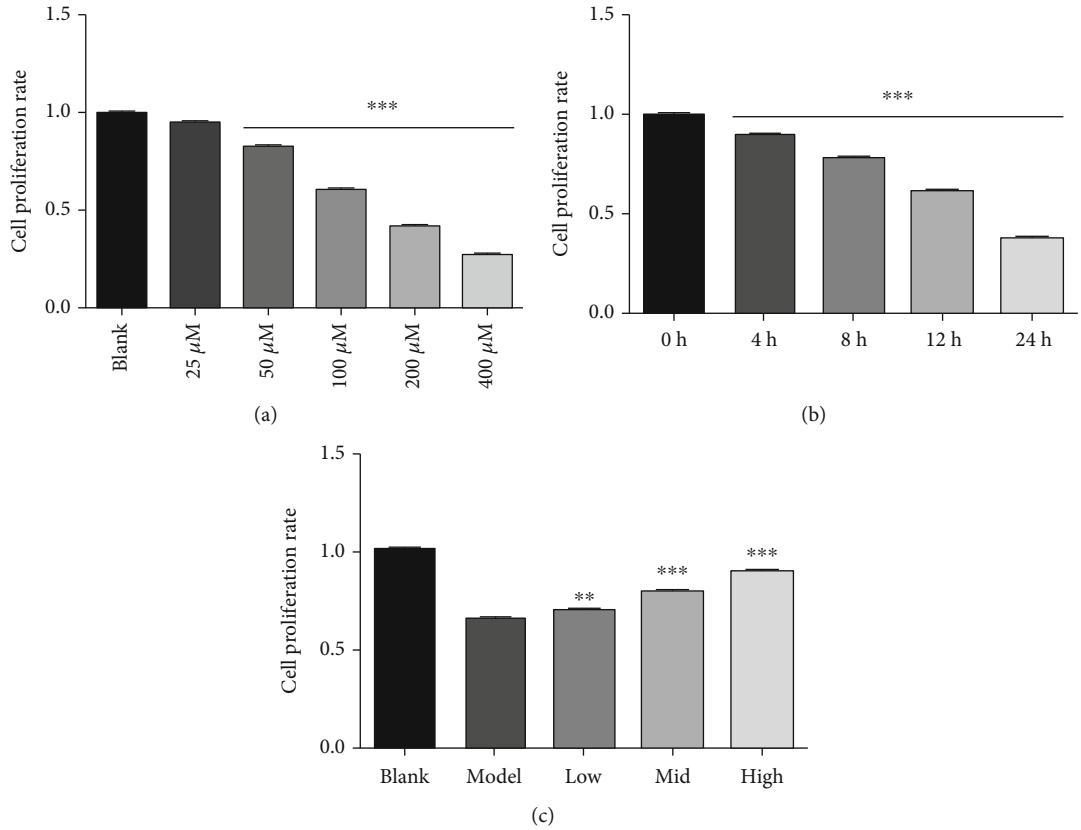

Figure 3: Cell viability (CCK-8) assay results of RLE-6TN cells. (a) H_2O_2-induced cell proliferation rate (concentration-dependent); (b) H_2O_2-induced cell proliferation rate (time-dependent); (c) 4,7-didehydro-neophysalin B treatment of the H_2O_2-challenged cells. Low: 2.5 μg/mL 4,7-didehydro-neophysalin B-treated RLE-6TN cell group; mid: 5 μg/mL 4,7-didehydro-neophysalin B-treated RLE-6TN cell group; high: 10 μg/mL 4,7-didehydro-neophysalin B-treated RLE-6TN cell group; the same as below. Compared with the blank group, $^{*}p < 0.05$, $^{**}p < 0.01$, and $^{***}p < 0.001$. Compared with the model group, $^{\#}p < 0.05$, $^{\#\#}p < 0.01$, and $^{\#\#\#}p < 0.001$.

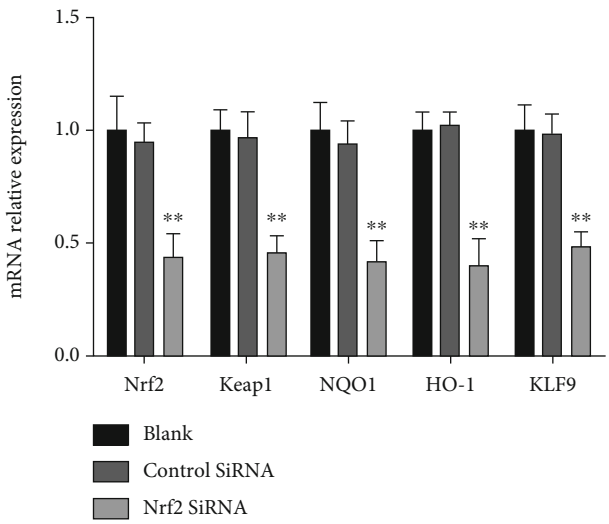

Figure 4: The mRNA expression of Nrf2 and its downstream genes. Compared with the blank group, $^{*}p < 0.05$ and $^{**}p < 0.01$.

< 0.001) as shown in Figure 3(a). Therefore, 100 μmol H_2O_2 was selected as a working concentration.

Compared with the blank group, the working time for 100 μmol H_2O_2 in RLE-6TN cells treated with different times was determined. The results showed that RLE-6TN cells treated with 100 μmol H_2O_2 for 24, 12, 8, and 4 h treatment all had significant effect on cell viability, but the RLE-6TN cells treated with 100 μmol H_2O_2 for 24 ($37.84 \pm 1.62\%$, $p = 0.0005 < 0.001$), 8 ($76.62 \pm 1.45\%$, $p = 0.0006 < 0.001$), and 4 ($87.61 \pm 2.33\%$, $p = 0.0009 < 0.001$) hours were too high or low on cell viability, as shown in Figure 3(b). Therefore, 12 h ($68.88 \pm 0.95\%$, $p = 0.0002 < 0.001$) was selected as a working time.

Conclusively, 100 μmol of H_2O_2 was used to treat RLE-6TN for 12 h, followed by the addition of 4,7-didehydro-neophysalin B to examine the effect on cell viability. As shown in Figure 3(c), 4,7-didehydro-neophysalin B had significantly reversed the cell viability caused by H_2O_2 in a dose-dependent manner in which 10 μg/mL 4,7-didehydro-neophysalin B showed the strongest effect ($84.93 \pm 1.86\%$, $p = 0.0007 < 0.001$).

3.4. Expressions of Nrf2 in RLE-6TN under the Intervention of Nrf2's siRNA. The mRNA expression of Nrf2 and its downstream genes was detected by RT-PCR. The A_{260}/A_{280} ratio of the RNA samples was 1.8-2.0. Nrf2's siRNA treatment significantly reduced the mRNA expression of Nrf2 and its downstream genes compared with the control siRNA

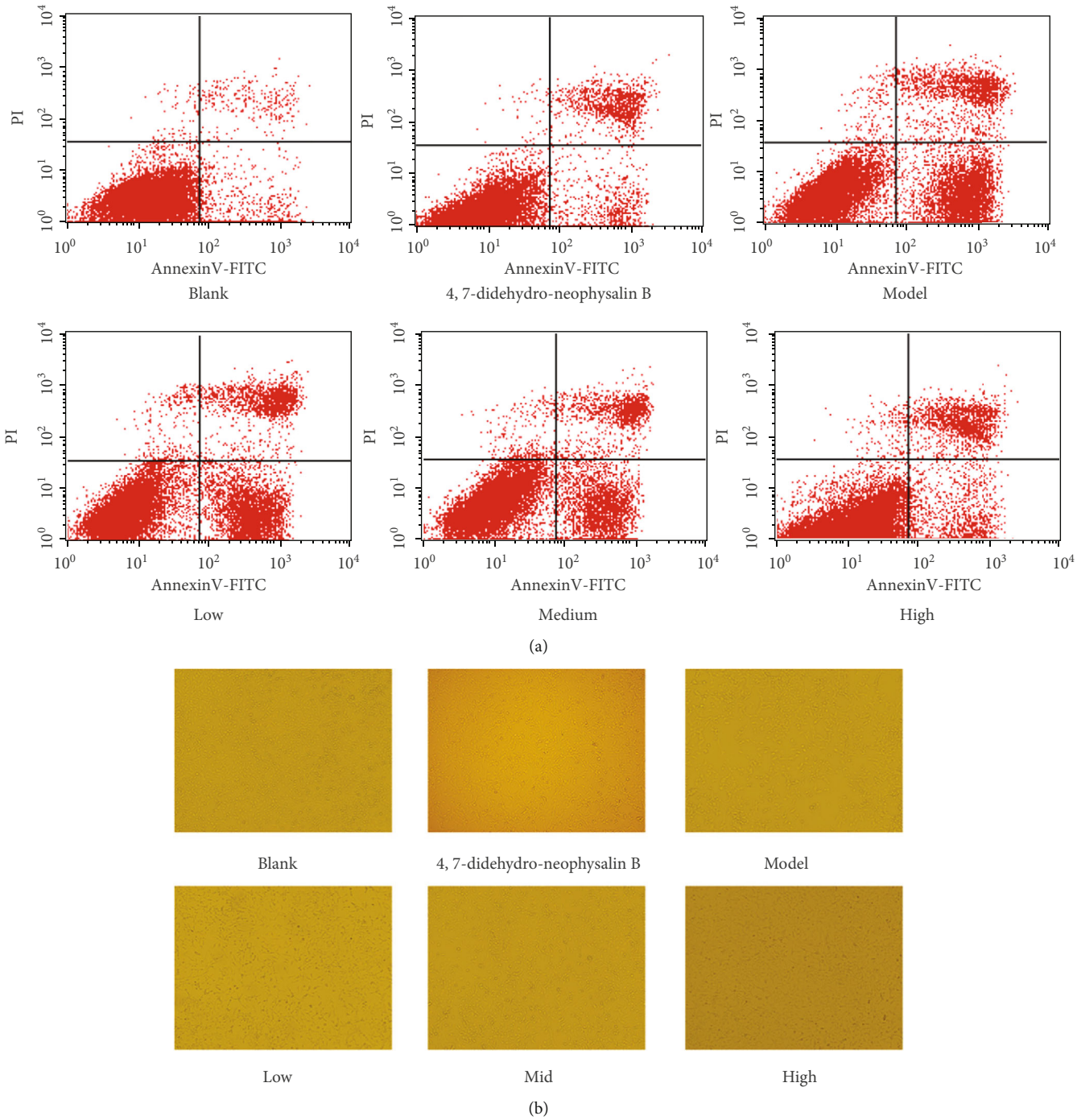

Figure 5: (a) The effect of 4,7-didehydro-neophysalin B on H_2O_2-induced apoptosis in RLE-6TN cells. (b) The microscope images of H_2O_2-induced cells after treatment with 4,7-didehydro-neophysalin B.

which have shown negligible effect on the mRNA expression of Nrf2 and its downstream genes, as shown in Figure 4.

3.5. 4,7-Didehydro-neophysalin B Mitigates H_2O_2-Induced Apoptosis in RLE-6TN. We investigated the effect of 4,7-didehydro-neophysalin B on H_2O_2-induced cell apoptosis by flow cytometry. Compared with the blank group, H_2O_2 caused a significant increase in RLE-6TN cell apoptosis while only 4,7-didehydro-neophysalin B treatment showed no significant effect on cell viability. Similarly, 4,7-didehydro-neophysalin B treatment dramatically mitigated H_2O_2-induced apoptosis. These results elucidated that 4,7-didehydro-neophysalin B had only a significant effect on H_2O_2-induced early apoptosis but had no significant effect on late apoptosis (early apoptosis: 4,7-didehydro-neophysalin B group $7.98 \pm 1.15\%$, $p = 0.07 > 0.05$; model group $37.48 \pm 3.84\%$, $p = 0.0005 < 0.001$; low-dose group $29.83 \pm 3.68\%$, $p = 0.0007 < 0.001$; medium-dose group $21.44 \pm 2.99\%$, $p =$

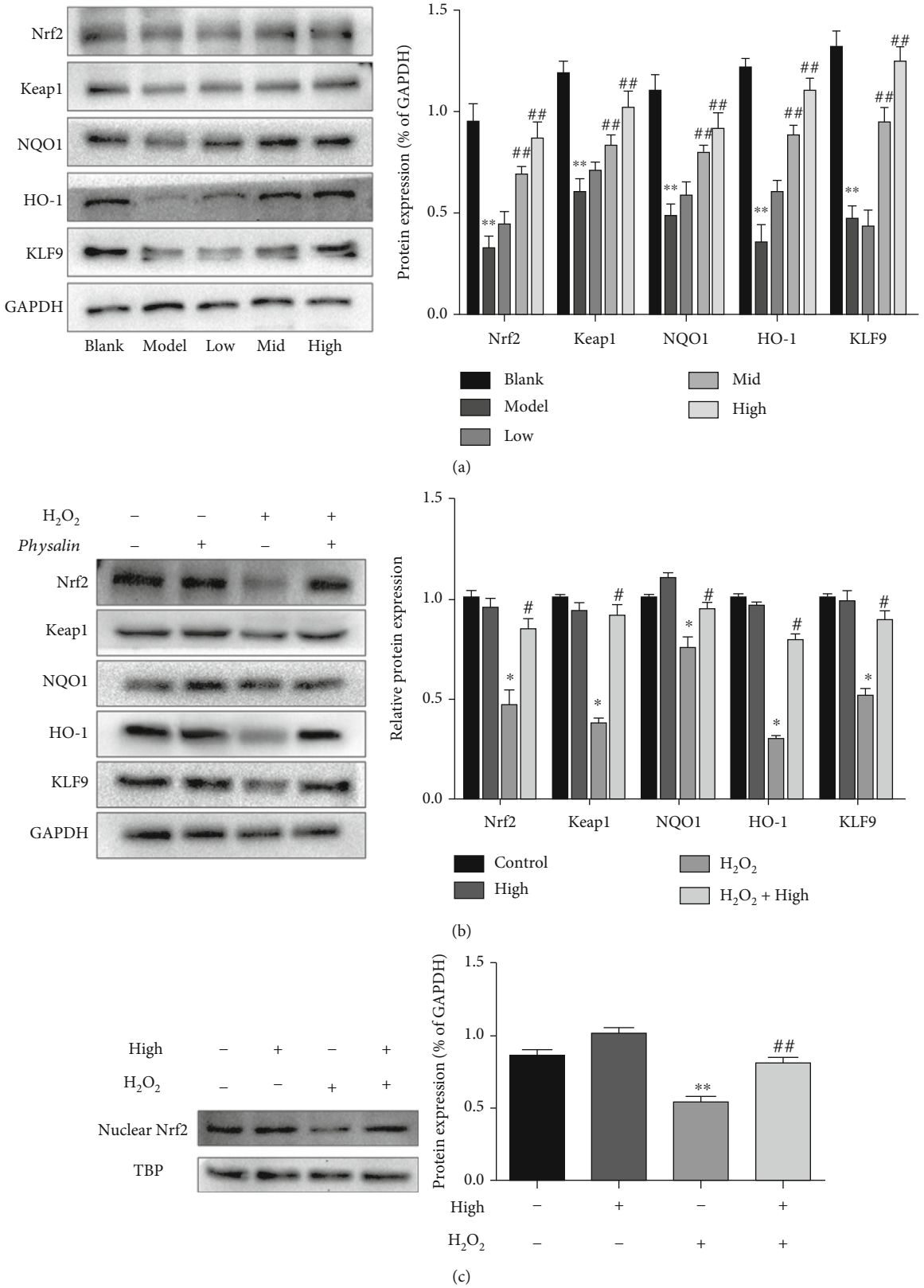

Figure 6: Western blot analysis of the Nrf2 signaling pathway. (a) After being added with different concentrations of 4,7-didehydro-neophysalin B, Nrf2 pathway-related protein expression in RLE-6TN cells and its quantitative band intensity analysis. (b) Effect of 4,7-didehydro-neophysalin B on the expression of Nrf2 pathway-related proteins and the quantitative band intensity analysis. (c) Expression of Nrf2 protein in the nucleus and its quantitative band intensity analysis. Compared with the blank group, $^{*}p < 0.05$, $^{**}p < 0.01$, and $^{***}p < 0.001$. Compared with the H_2O_2+0% 4,7-didehydro-neophysalin B group, $^{\#}p < 0.05$, $^{\#\#}p < 0.01$, and $^{\#\#\#}p < 0.001$.

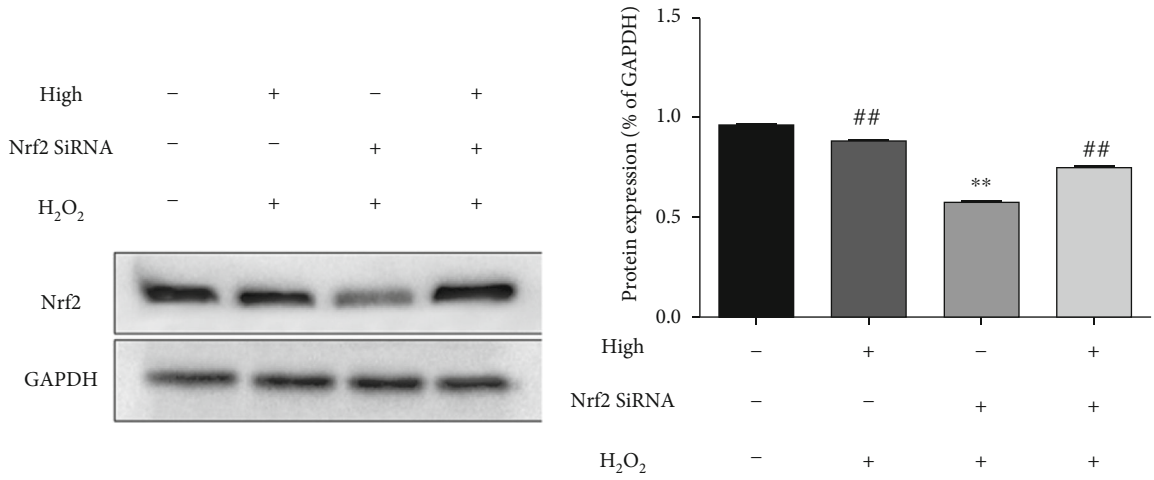

Figure 7: After using Nrf2 siRNA to knock down the expression of Nrf2 protein, effect of 4,7-didehydro-neophysalin B on the expression of Nrf2 pathway-related proteins and their quantitative band intensity analysis. Compared with the blank group, $^{*}p < 0.05$ and $^{**}p < 0.01$. Compared with the H_2O_2+0% 4,7-didehydro-neophysalin B group, $^{\#}p < 0.05$ and $^{\#\#}p < 0.01$.

$0.0008 < 0.001$; high-dose group $15.35 \pm 1.68\%$, $p = 0.03 < 0.05$, compared with the blank group) (late apoptosis: 4,7-didehydro-neophysalin B group $13.32 \pm 2.47\%$, $p = 0.008 < 0.01$; model group $24.49 \pm 2.96\%$, $p = 0.006 < 0.01$; low-dose group $17.92 \pm 2.86\%$, $p = 0.007 < 0.01$; medium-dose group $15.58 \pm 3.15\%$, $p = 0.008 < 0.01$; high-dose group $19.44 \pm 3.57\%$, $p = 0.006 < 0.01$, compared with the blank group), as shown in Figure 5(a). The microscopic images of cells after treatment are shown in Figure 5(b).

3.6. The Effect of 4,7-Didehydro-neophysalin B on Nrf2-Dependent Signaling Pathway in H_2O_2-Induced Oxidative Damage. Nrf2 signaling pathway proteins were detected by western blotting. In vitro treatment of H_2O_2 significantly reduced the Nrf2, NQO1, Keap1, HO-1, and KLF9 protein expressions. However, 4,7-didehydro-neophysalin B treatment has significantly reversed these effects induced by H_2O_2 with 10 μg/mL 4,7-didehydro-neophysalin B showing the strongest effect as shown in Figure 6(a). The addition of 4,7-didehydro-neophysalin B alone showed no effect on the protein expression of Nrf2, NQO1, Keap1, HO-1, and KLF9 in RLE-6TN as shown in Figure 6(b). H_2O_2 had markedly reduced the expression of nuclear Nrf2 which was significantly reversed by 4,7-didehydro-neophysalin B as shown in Figure 6(c).

3.7. Knockdown of Nrf2 Declines the Treatment Effect of Physalin B. The Nrf2's siRNA treatment significantly reduced the expression of Nrf2 as shown in Figure 7. Compared with the model group, the treatment effect of 4,7-didehydro-neophysalin B in the Nrf2's siRNA treatment group was significantly reduced.

3.8. Effects of 4,7-Didehydro-neophysalin B on Bcl-2 Family and p53 Proteins. The molecular basis of a protective effect of 4,7-didehydro-neophysalin B against H_2O_2-induced cell apoptosis was investigated. H_2O_2 treatment decreased the expression of antiapoptotic Bcl-2 and Bcl-xL proteins in RLE-6TN cells. In H_2O_2-treated cells, 4,7-didehydro-neophysalin B administration significantly induced the expression of Bcl-2 and Bcl-xL. The expression of proapoptotic protein Bax was significantly increased post H_2O_2 treatment which was significantly reduced by 4,7-didehydro-neophysalin B treatment. Compared with the control group, p53 expression was also increased post H_2O_2 treatment. 4,7-Didehydro-neophysalin B attenuated H_2O_2-induced p53 expression with the strongest effect of 10 μg/mL 4,7-didehydro-neophysalin B as shown in Figure 8(a) (Bcl-xL expression: blank 1.0 ± 0.14, control 0.37 ± 0.05, $p = 0.004 < 0.01$ compared with the blank group; low 0.28 ± 0.07, mid 0.59 ± 0.09, $p = 0.03 < 0.05$ compared with the control group; high group 0.98 ± 0.05, $p = 0.11$ compared with the control group; Bcl-2 expression: blank 1.0 ± 0.16, control 0.48 ± 0.35, $p = 0.005 < 0.01$ compared with the model group; low 0.53 ± 0.005, mid 0.59 ± 0.77, $p = 0.04 < 0.05$ compared with the control group; high group 0.98 ± 0.05, $p = 0.11 < 0.01$ compared with the control group). The addition of 4,7-didehydro-neophysalin B alone showed no effect on the protein expression of Bcl-2, Bcl-xL, Bax, and p53 in RLE-6TN as shown in Figure 8(b).

4. Discussion

A variety of chemicals and environmental factors causes oxidative stress in the human body which damages and induces a variety of diseases. H_2O_2-induced RLE-6TN cell damage is a classical model of oxidative stress injury. Studies have shown that the damage caused by oxidative stress is mediated by reactive oxygen species which plays an important role in neurodegenerative diseases [20, 21]. H_2O_2 produced in the body during metabolism is equivalent to reactive oxygen species and can aggravate the body oxidative stress injury [22, 23]. The results of this study showed that H_2O_2 induced oxidative damage and apoptosis in RLE-6TN cells which was reduced by 4,7-didehydro-neophysalin B treatment as shown in Figure 2(c). This study demonstrated that

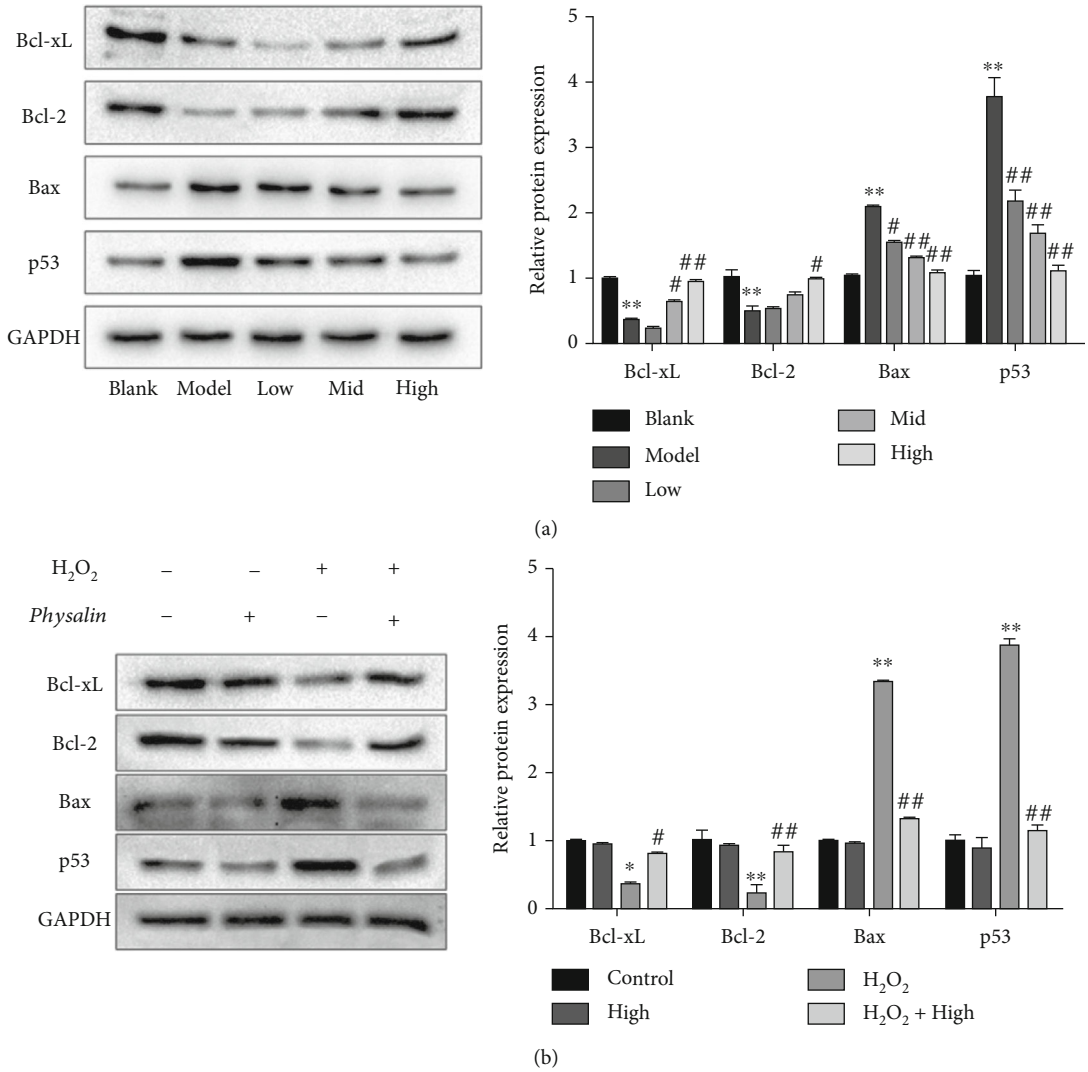

Figure 8: Western blot analysis of p53 pathway protein. (a) Post addition of different 4,7-didehydro-neophysalin B concentrations, p53 pathway-related protein expression in RLE-6TN cells and their quantitative band intensity analysis. (b) Effect of 4,7-didehydro-neophysalin B on the expression of p53 pathway-related proteins and the quantitative band intensity analysis. Compared with the blank group, $^{*}p < 0.05$ and $^{**}p < 0.01$, and with the H_2O_2+0% 4,7-didehydro-neophysalin B group, $^{\#}p < 0.05$ and $^{\#\#}p < 0.01$.

4,7-didehydro-neophysalin B possessed therapeutic effects in the form of antioxidant activities against H_2O_2-induced oxidative stress injury.

When the cellular level of ROS exceeds the body's antioxidant capacity, it induces oxidative stress leaving the cells in a redox state by producing peroxides and free radicals [24–26]. Mitochondrial dysfunction and DNA damage are caused by the accumulation of reactive oxygen species which mediate and accelerate apoptosis [27–30]. DNA damage causes activation of p53which serves as a major mediator of cellular stress [31]. Our results (Figure 7) indicated p53-mediated apoptosis in H_2O_2-induced lung injury. p53 along with the members of Bcl-2 family proteins regulates protein–protein interactions and causes activation of Bax which promotes mitochondrial membrane permeability and hence induces apoptosis [32]. In this study, 4,7-didehydro-neophysalin B suppressed p53, decreased the level of proapoptotic member Bax, and increased the level of prosurvival members Bcl-2 and Bcl-xL. Moreover, the results of apoptotic index (Figure 2) and cell viability (Figure 4) of RLE-6TN were consistent with the observed effects on Bcl-2 family proteins. These findings suggest that 4,7-didehydro-neophysalin B has a pivotal role in regulating apoptosis and inhibiting oxidative stress-induced cell death. It is also noteworthy that some studies showed that NQO1 stabilizes the tumor suppressor p53 [33]. HO-1 upregulates Bcl-2 and Bcl-xL expressions [34] which are downstream proteins of Nrf2. A possible explanation is that 4,7-didehydro-neophysalin B protects lung injury induced by H_2O_2 via activating the Nrf2 pathway.

The transcription factor Nrf2 plays an important role in protection against oxidative damage [35, 36]. Nrf2 senses the presence of oxidative stress and regulates transcription of genes encoding cytoprotective enzymes and other proteins crucial for maintaining cellular homeostasis. Under physiological conditions, the Nrf2 inhibitor, Keap-1, which is a

negative regulator of Nrf2 binds to Nrf2 and retains Nrf2 in the cytoplasm [37]. During oxidative stress, Nrf2 dissociates from Keap1, translocates into the nucleus, and activates ARE-dependent gene expression including transcription of target genes NQO-1 and HO-1 [38], thereby improving the antioxidant capacity in the body [39, 40]. Accumulation of Nrf2 in the nucleus is a necessary condition which is closely related to the induction of cellular defense genes [41]. The increase in cell death caused by H_2O_2 might be attributed to the insufficient ROS removal caused by the failure of Nrf2 activation. However, Figure 5 shows that 4,7-didehydro-neophysalin B activates the antioxidant pathway affecting both Nrf2 gene levels and expression of its target proteins. Therefore, this study suggested that Nrf2 activation was required for protection of the lungs by 4,7-didehydro-neophysalin B from H_2O_2-mediated cell death.

5. Conclusions

In conclusion, our study demonstrated that *Physalin* B attenuated H_2O_2-induced lung injury by regulating the Nrf2/P53 signaling pathway. *Physalin* B with great therapeutical potential can be used as an antioxidant agent. This study provided beneficial evidences for the application of *Physalin* B supplementation as an alternative treatment strategy for lung injury.

Abbreviations

H_2O_2: Hydrogen peroxide
ROS: Reactive oxygen species
Nrf2: Nuclear translocation of erythroid-2-related factor 2
PVDF: Polyvinylidene fluoride
GAPDH: Glyceraldehyde-3-phosphate dehydrogenase
ARE: Antioxidant response element
TBP: TATA-binding protein
HO-1: Heme oxygenase-1
NQO1: Nicotinamide adenine dinucleotide phosphatase:quinone-acceptor 1
KLF9: Krueppel-like factor 9
Keap-1: Kelch-like ECH-associated protein
Bax: Bcl-2-associated X protein
Bcl-2: B cell lymphoma gene 2
Bcl-xL: B cell lymphoma-extra large
SEM: Standard errors of the mean.

Data Availability

The original contributions presented in the study are included in the article; further inquiries can be directed to the corresponding author.

Conflicts of Interest

The authors declare that there is no conflict of interest regarding the publication of this paper.

Authors' Contributions

Conceptualization and methodology were done by Qiu Zhong and Yao-gui Sun; investigation, data curation, and writing—original draft preparation were done by Qiu Zhong; validation was done by Qiu Zhong and Yao-gui Sun; writing—review and editing were done by Ajab Khan, Jianhua Guo, Zhirui Wang, and Na Sun; funding acquisition was done by Yaogui Sun and Hongquan Li; project administration was done by Hongquan Li. All authors have read and agreed to the reviewed version of the manuscript.

Acknowledgments

This work was supported by the Key Research and Development Plan of Shanxi Province (grant numbers 202102140601019 and 201803D221023-3).

References

[1] C. C. Winterbourn, "Biological production, detection and fate of hydrogen peroxide," *Antioxidants & Redox Signaling*, vol. 29, no. 6, pp. 541–551, 2018.

[2] Q. Liu, Y. Gao, and X. Ci, "Role of Nrf2 and its activators in respiratory diseases," *Oxidative Medicine & Cellular Longevity*, vol. 2019, article 7090534, 17 pages, 2019.

[3] W. Hou, X. Xu, Y. Lei et al., "The role of the PM2.5-associated metals in pathogenesis of child Mycoplasma pneumoniae infections: a systematic review," *Environmental Science & Pollution Research*, vol. 23, no. 11, pp. 10604–10614, 2016.

[4] G. Sun, X. Xu, Y. Wang, X. Shen, Z. Chen, and J. Yang, "Mycoplasma pneumoniae infection induces reactive oxygen species and DNA damage in A549 human lung carcinoma cells," *Infection & Immunity*, vol. 76, no. 10, pp. 4405–4413, 2008.

[5] L. Wei, W. Zhong, T. Sun et al., "Proteomic and mechanistic study of Qingxuan Tongluo formula and curcumin in the treatment of Mycoplasma pneumoniae pneumonia - ScienceDirect," *Biomedicine & Pharmacotherapy*, vol. 133, article 110998, 2021.

[6] C. Schott, H. Cai, L. Parker, K. G. Bateman, and J. L. Caswell, "Hydrogen peroxide production and free radical-mediated cell stress in _Mycoplasma bovis_ pneumonia," *Journal of Comparative Pathology*, vol. 150, no. 2-3, pp. 127–137, 2014.

[7] M. D. S. Lima, A. F. Evangelista, G. G. L. D. Santos et al., "Antinociceptive properties of physalins from Physalis angulata," *Journal of Natural Products*, vol. 77, no. 11, pp. 2397–2403, 2014.

[8] A. L. Li, B. J. Chen, G. H. Li et al., "Physalis alkekengi L. var. franchetii (Mast) Makino: an ethnomedical, phytochemical and pharmacological review," *Journal of Ethnopharmacology*, vol. 210, pp. 260–274, 2018.

[9] D. P. Castro, C. S. Moraes, M. S. Gonzalez et al., "Physalin B inhibits _Trypanosoma cruzi_ infection in the gut of _Rhodnius prolixus_ by affecting the immune system and microbiota," *Journal of Insect Physiology*, vol. 58, no. 12, pp. 1620–1625, 2012.

[10] Y. Yu, L. Sun, L. Ma, J. Li, L. Hu, and J. Liu, "Investigation of the immunosuppressive activity of physalin H on T lymphocytes," *International Immunopharmacology*, vol. 10, no. 3, pp. 290–297, 2010.

[11] C. Yang, Y.-x. Tan, G.-z. Yang et al., "IL-6 promotes the differentiation of a subset of naive CD8+ T cells into IL-21-producing B helper CD8+ T cells," *Journal of Experimental Medicine*, vol. 213, no. 11, pp. 2281–2291, 2016.

[12] C. Diao, Z. Chen, T. Qiu, H. Liu, and L. Wang, "Inhibition of PRMT5 attenuates oxidative stress-induced pyroptosis via activation of the Nrf2/HO-1 signal pathway in a mouse model of renal ischemia- reperfusion injury," *Oxidative Medicine and Cellular Longevity*, vol. 2019, Article ID 2345658, 18 pages, 2019.

[13] J. Ge, C. Zhang, Y.-C. Sun et al., "Cadmium exposure triggers mitochondrial dysfunction and oxidative stress in chicken (_Gallus gallus_) kidney via mitochondrial UPR inhibition and Nrf2-mediated antioxidant defense activation," *Science of the Total Environment*, vol. 689, pp. 1160–1171, 2019.

[14] Y. Zhang, D. Yuan, W. Yao et al., "Hyperglycemia aggravates hepatic ischemia reperfusion injury by inducing chronic oxidative stress and inflammation," *Oxidative Medicine & Cellular Longevity*, vol. 2016, article 3919627, 16 pages, 2016.

[15] L. Wu, Y. Cen, M. Feng, Y. Zhou, and M. Zhou, "Metformin activates the protective effects of the AMPK pathway in acute lung injury caused by paraquat poisoning," *Oxidative Medicine and Cellular Longevity*, vol. 2019, Article ID 1709718, 10 pages, 2019.

[16] K. E. Driscoll, L. C. Deyo, J. M. Carter, B. W. Howard, D. G. Hassenbein, and T. A. Bertram, "Effects of particle exposure and particle-elicited inflammatory cells on mutation in rat alveolar epithelial cells," *Carcinogenesis*, vol. 18, no. 2, pp. 423–430, 1997.

[17] Q. Zhong, Y. Sun, Y. Xu et al., "The therapeutic effect and mechanism of physalin on LPS-induced acute lung injury in rats," *Pakistan Veterinary Journal*, vol. 41, no. 3, pp. 372–378, 2021.

[18] D. Xue, X. Zhou, and J. Qiu, "Cytotoxicity mechanisms of plumbagin in drug-resistant tongue squamous cell carcinoma," *Journal of Pharmacy and Pharmacology*, vol. 73, no. 1, pp. 98–109, 2021.

[19] V. Rubovitch, S. Gershnabel, and M. Kalina, "Lung epithelial cells modulate the inflammatory response of alveolar macrophages," *Inflammation*, vol. 30, no. 6, pp. 236–243, 2007.

[20] L. H. You, Z. Li, X. L. Duan, B. L. Zhao, Y. Z. Chang, and Z. H. Shi, "Mitochondrial ferritin suppresses MPTP-induced cell damage by regulating iron metabolism and attenuating oxidative stress," *Brain Research*, vol. 1642, pp. 33–42, 2016.

[21] J. Karolina, D. Karolina, K. Justyna, K. Dorota, K. Joanna, and J. Katarzyna, "Reactive oxygen species - sources, functions, oxidative damage," *Polski merkuriusz lekarski : organ Polskiego Towarzystwa Lekarskiego*, vol. 48, no. 284, pp. 124–127, 2020.

[22] Y. Ma, D. Wu, X. Ding, and W. Ying, "CD38 plays key roles in both antioxidation and cell survival of H_2O_2-treated primary rodent astrocytes," *International Journal of Physiology Pathophysiology & Pharmacology*, vol. 6, no. 2, pp. 102–108, 2014.

[23] L. E. Volk, C. D. Mavroudis, T. Ko, T. Hallowell, and T. J. Kilbaugh, "Increased cerebral mitochondrial dysfunction and reactive oxygen species with cardiopulmonary bypass," *European Journal of Cardio-Thoracic Surgery*, vol. 59, no. 6, pp. 1256–1264, 2021.

[24] P. Yao, X. Chen, Y. Yan et al., "Glutaredoxin 1, glutaredoxin 2, thioredoxin 1, and thioredoxin peroxidase 3 play important roles in antioxidant defense in Apis cerana cerana," *Free Radical Biology and Medicine*, vol. 68, pp. 335–346, 2014.

[25] Y. C. Yang, C. K. Lii, A. H. Lin et al., "Induction of glutathione synthesis and heme oxygenase 1 by the flavonoids butein and phloretin is mediated through the ERK/Nrf2 pathway and protects against oxidative stress," *Free Radical Biology & Medicine*, vol. 51, no. 11, pp. 2073–2081, 2011.

[26] J. M. Brown, J. G. Ball, M. S. Wright, S. V. Meter, and M. A. Valentovic, "Novel protective mechanisms for S-adenosyl-l-methionine against acetaminophen hepatotoxicity: improvement of key antioxidant enzymatic function," *Toxicology Letters*, vol. 212, no. 3, pp. 320–328, 2012.

[27] S. Choudhury, S. Ghosh, S. Mukherjee et al., "Pomegranate protects against arsenic-induced p53-dependent ROS-mediated inflammation and apoptosis in liver cells," *Journal of Nutritional Biochemistry*, vol. 38, pp. 25–40, 2016.

[28] H. Lv, Q. Liu, J. Zhou, G. Tan, X. Deng, and X. Ci, "Daphnetin-mediated Nrf2 antioxidant signaling pathways ameliorate tert-butyl hydroperoxide (_t_-BHP)-induced mitochondrial dysfunction and cell death," *Free Radical Biology & Medicine*, vol. 106, pp. 38–52, 2017.

[29] Z. Zhang, S. Li, H. Jiang et al., "Effects of selenium on apoptosis and abnormal amino acid metabolism induced by excess fatty acid in isolated rat hepatocytes," *Molecular Nutrition & Food Research*, vol. 61, no. 9, article 1700016, 2017.

[30] S. Li, X. Zheng, X. Zhang et al., "Exploring the liver fibrosis induced by deltamethrin exposure in quails and elucidating the protective mechanism of resveratrol," *Ecotoxicology and Environmental Safety*, vol. 207, article 111501, 2021.

[31] M. Li, X. Tian, L. Xu, R. An, and M. Yang, "β-Caryophyllene pretreatment alleviates focal cerebral ischemia-reperfusion injury by activating PI3K/Akt signaling pathway," *Neurochemical Research*, vol. 42, no. 5, pp. 1459–1469, 2017.

[32] D. Speidel, "The role of DNA damage responses in p53 biology," *Archives of Toxicology*, vol. 89, no. 4, pp. 501–517, 2015.

[33] H. Zhu and Y. Li, "NAD(P)H:quinone oxidoreductase 1 and its potential protective role in cardiovascular diseases and related conditions," *Cardiovascular Toxicology*, vol. 12, no. 1, pp. 39–45, 2012.

[34] B. Ke, X. D. Shen, F. Gao et al., "Small interfering RNA targeting heme oxygenase-1 (HO-1) reinforces liver apoptosis induced by ischemia–reperfusion injury in mice: HO-1 is necessary for cytoprotection," *Human Gene Therapy*, vol. 20, no. 10, pp. 1133–1142, 2009.

[35] L. Zeng, C.-W. Wu, J.-L. Zheng, M.-Y. Xu, and A.-Y. Zhu, "The role of Nrf2/Keap1 signaling in inorganic mercury induced oxidative stress in the liver of large yellow croaker _Pseudosciaena crocea_," *Ecotoxicology and Environmental Safety*, vol. 132, pp. 345–352, 2016.

[36] D. Yang, Z. Lv, H. Zhang et al., "Activation of the Nrf2 signaling pathway involving KLF9 plays a critical role in allicin resisting against arsenic trioxide-induced hepatotoxicity in rats," *Biological Trace Element Research*, vol. 176, no. 1, pp. 192–200, 2017.

[37] A. Wang, S. Wang, Y. Jiang, M. Chen, Y. Wang, and L. Lin, "Bio-assay guided identification of hepatoprotective polyphenols from Penthorum chinense Pursh on t-BHP induced oxidative stress injured L02 cells," *Food & Function*, vol. 7, no. 12, pp. 4956–4966, 2016.

[38] P. Ray, B. W. Huang, and Y. Tsuji, "Reactive oxygen species (ROS) homeostasis and redox regulation in cellular signaling," *Cellular Signalling*, vol. 24, no. 5, pp. 981–990, 2012.

[39] H. K. Na and Y. J. Surh, "Oncogenic potential of Nrf2 and its principal target protein heme oxygenase-1," *Free Radical Biology & Medicine*, vol. 67, pp. 353–365, 2014.

[40] G. S. Oh, H. J. Kim, J. H. Choi et al., "Pharmacological activation of NQO1 increases NAD^+ levels and attenuates cisplatin-mediated acute kidney injury in mice," *Kidney International*, vol. 85, no. 3, pp. 547–560, 2014.

[41] M. S. Joo, W. D. Kim, K. Y. Lee, J. H. Kim, J. H. Koo, and S. G. Kim, "AMPK facilitates nuclear accumulation of Nrf2 by phosphorylating at serine 550," *Molecular & Cellular Biology*, vol. 36, no. 14, pp. 1931–1942, 2016.